Title
Regional brain tissue integrity in pediatric obstructive sleep apnea

Authors
Kheirandish-Gozal, Leila
Sahib, Ashish K
Macey, Paul M
et al.

Publication Date
2018-08-01

DOI
10.1016/j.neulet.2018.06.002

Peer reviewed

HHS Public Access

Author manuscript

Neurosci Lett. Author manuscript; available in PMC 2019 August 24.

Published in final edited form as:

Neurosci Lett. 2018 August 24; 682: 118–123. doi:10.1016/j.neulet.2018.06.002.

Regional Brain Tissue Integrity in Pediatric Obstructive Sleep Apnea

Leila Kheirandish-Gozal[1], **Ashish K. Sahib**[2], **Paul M. Macey**[3,6], **Mona F. Philby**[1], **David Gozal**[1], and **Rajesh Kumar**[2,4,5,6,*]

[1]Section of Pediatric Sleep Medicine, Department of Pediatrics, Pritzker School of Medicine, Biological Sciences Division, University of Chicago, Chicago, IL, USA

[2]Department of Anesthesiology, University of California Los Angeles, Los Angeles, CA 90095, USA

[3]Department of UCLA School of Nursing, University of California Los Angeles, Los Angeles, CA 90095, USA

[4]Department of Radiological Sciences, University of California Los Angeles, Los Angeles, CA 90095, USA

[5]Department of Bioengineering, University of California Los Angeles, Los Angeles, CA 90095, USA

[6]Department of Brain Research Institute, University of California Los Angeles, Los Angeles, CA 90095, USA

Abstract

Children with long-standing obstructive sleep apnea (OSA) show evidence of neural injury and functional deficits in behavioral and cognitive regulatory brain regions that are reflected in symptoms of altered cognitive performance and behaviors. While we earlier showed reduced gray matter volume and increased and reduced regional cortical thicknesses, such structural changes give little indication of the underlying pathology. Brain tissue integrity in pediatric OSA subjects can reflect the nature and extent of injury or structural adaptation, and can be assessed by entropy tissue texture, a measure of local changes in signal intensity patterns from high-resolution magnetic resonance images. We collected high-resolution T1-weighted magnetic resonance images from 10 pediatric OSA (age, 7.9±1.1 years; apnea-hypopnea-index, 8.8±3.0 events/hour; body-mass-index, 20±6.7 kg/m^2; 7 male) and 8 healthy controls (age, 8.8±1.6 years; body-mass-index, 19.6±5.9 kg/m^2; 5 female). Images were bias-corrected and entropy maps calculated, individual maps were normalized to a common space, smoothed, and compared between groups (ANCOVA; covariates: age, gender; SPM12, uncorrected-threshold $p<0.005$). No significant

*Address for Correspondence: Rajesh Kumar, PhD, Department of Anesthesiology, David Geffen School of Medicine at UCLA, 56-141 CHS, 10833 Le Conte Ave, University of California at Los Angeles, Los Angeles, CA 90095-1763, USA, Tel: 310-206-6133; 310-206-1679, Fax: 310-825-2236, rkumar@mednet.ucla.edu.

differences in age (p=0.48), gender (p=0.59), or body-mass-index (p=0.63) emerged between groups. In OSA children, several brain sites including the pre-frontal cortex, middle and posterior corpus callosum, thalamus, hippocampus, and cerebellar areas showed reduced entropy values, indicating tissue changes suggestive of acute insults. No regions showed higher entropy values in OSA. Children suffering from OSA display predominantly acute tissue injury in neural regions principally localized within autonomic, respiratory, cognitive, and neuropsychologic control, functions that correspond to previously-reported comorbidities associated with OSA. A range of acute processes, including hypoxia/re-oxygenation, repeated arousals, and episodic hypercarbia, may have contributed to regional brain tissue integrity changes in pediatric OSA.

Keywords

Entropy; Acute injury; Insula; Cingulate; Hippocampus

1. INTRODUCTION

Pediatric obstructive sleep apnea (OSA) has been widely recognized as a likely causal contributor to a significant array of morbidities in children [1]. The condition is characterized by increased upper airway resistance during sleep, leading to altered oxygenation and hypercapnia, as well as repeated arousals, sleep fragmentation, and reduced sleep efficiency [2]. Children with OSA exhibit increased risk of cognitive and behavioral deficits that may adversely impact their healthy development, including difficulties maintaining academic performance [1, 3, 4]. A possible source of these symptoms in OSA could be brain alterations, which have been shown in selected regions via magnetic resonance imaging [5–7].

Multiple animal studies have conclusively shown that both intermittent hypoxia and sleep fragmentation mimicking OSA lead to neuronal cell losses in several brain regions, particularly in the developing brain [8, 9]. In addition, studies in pediatric OSA cohorts have reported reduced gray matter volumes, increased and decreased regional cortical thickness, and tissue diffusion changes in neural sites putatively underlying cognitive and executive deficits [5, 7, 10]. However, limited sensitivity from the inherent small range of values on gray matter volume assessment and spatial resolution issues on other MRI imaging precluded insights into the nature and extent of whole-brain tissue integrity. The latter can however be readily examined with tissue texture assessments using high-resolution T1-weighted images, which is sensitive to nature and extent of tissue changes, with more homogenous texture associated with acute alterations [11]. The assessment of whole-brain changes as tissue texture could elucidate mechanisms of brain structural alterations in children suffering from OSA.

Tissue texture is a type of measure that quantifies spatial patterns of image signal intensities that differ with the variable nature and extent of brain tissue injury [12]. Among the several tissue texture measures, entropy measures the extent of homogeneity or randomness based on signal intensity characteristics, and values are inversely proportional to the amount of free water content in the tissue [13], such that decreased extracellular water corresponds to cell

and axonal swelling [14]. We hypothesized that compared to healthy children, regional brain entropy values would be reduced in pediatric OSA patients in various autonomic, cognitive, and mood control areas, and therefore, be indicative of brain injury. Accordingly, our aim was to investigate the nature and extent of whole-brain tissue integrity based on entropy measures using high-resolution T1-weighted imaging in pediatric OSA subjects and controls.

2. MATERIALS AND METHODS

2.1 Subjects

Ten children with polysomnographically-confirmed OSA and 8 healthy control subjects of similar ages and genders without any evidence of sleep-disordered breathing in an overnight sleep study were included in this study. Demographic and other variables are summarized in Table 1. All OSA and control subjects were initially habituated to the MRI scanner environment using a mock replica. None of the children were taking psychostimulants or anti-hypertensive medications, and subjects had no history of neurodevelopmental disorders, suspected diabetes, or any other known acute or chronic illness. The study was approved by the human subject committee at the University of Chicago (protocol #11-0280-CR009), and informed consent and assent were obtained from each participant's legal caregiver and child, respectively. Furthermore, three additional controls were recruited at the University of California at Los Angeles (UCLA) campus, after obtaining informed consent from parents, and those data collection procedures were carried out with UCLA Institutional Review Board approval.

2.1.1 Anthropometry—Height and weight were measured and body mass index (BMI) z-scores were calculated using the Center Children's Hospital of Philadelphia online software (http://stokes.chop.edu/web/zscore). A BMI z-score >1.65 was considered as obesity.

2.1.2 Overnight Polysomnography—Overnight polysomnography studies were conducted and scored using previously-described standard approaches [15, 16]. An obstructive apnea-hypopnea (AHI) >2 events/hour along with a nadir oxygen saturation < 92% and/or a respiratory arousal index >2 events/hour served as criteria for OSA diagnosis [17, 18].

2.2 MRI scanning

Five control and 10 OSA subjects were scanned at 1.5-Tesla (Philips Achieva) within 3 – 5 days after the sleep study. High-resolution T1-weighted anatomical scans were collected using a custom ultrafast gradient echo "SENSE" sequence [repetition-time (TR) = 8.16 ms; echo-time (TE) = 3.7 ms; flip-angle (FA) = 8°; matrix size = 256 × 256; field-of-view (FOV) = 224×224 mm^2; slice thickness = 1.0 mm; slices = 160]. The three additional UCLA control subjects were scanned at 3.0-Tesla (Siemens, Magnetom Trio). High-resolution T1-weighted images were collected using a magnetization prepared rapid acquisition gradient-echo sequence (TR = 2200 ms; TE = 3.05 ms; inversion time = 1100 ms; FA = 10°; matrix size = 256×256; FOV = 220×220 mm^2; slice thickness = 1.0 mm; slices = 176).

2.3 Data Processing and Analysis

Various software tools were used for image visualization, data pre-processing, and analyses, and included the statistical parametric mapping package SPM12 (Well-come Department of Cognitive Neurology, UK; http://www.fil.ion.ucl.ac.uk/spm), MRIcroN [19], and MATLAB-based custom routines (The MathWorks Inc, Natick, MA). T1-weighted images of all OSA and control subjects were visually-examined to ensure that no serious brain pathologies (e.g., cyst, tumor, and infarct) were present.

2.3.1 Entropy Calculation—High-resolution T1-weighted images were bias corrected to remove any signal intensity variations due to field inhomogeneities using SPM 12 [20]. Using the bias-corrected T1-weighted images, the entropy values at a given voxel '*v*' were calculated with the following equation by defining a 3×3×3 volume of interest (VOI) with '*v*' as center:

$$E = -\sum_{i=1}^{N} p_i \log(p_i)$$

Where, N is number of distinct pixel values (gray/white matter) in the VOI, and p_i is probability of occurrence of i^{th} pixel value in the VOI. Mathematically, the VOI can be represented as below:

$$\mathrm{VOI} = \mathrm{I}(\mathrm{x}-1.5{:}\mathrm{x}+1.5, \mathrm{y}-1.5{:}\mathrm{y}+1.5, \mathrm{z}-1.5{:}\mathrm{z}+1.5)$$

Where, 'I' is the bias corrected T1-weighted image, and x, y, z are spatial coordinates.

2.3.2 Normalization and Smoothing of Entropy Maps—Before normalization, the entropy values were scaled between 0–1 by dividing the whole-brain entropy by its maximum value, to attain a common distribution of entropy values across the scanners. Whole-brain entropy maps were then normalized to Montreal Neurological Institute (MNI) space using the SPM12 package. The warping parameters for *x, y, z* directions were obtained from the bias-corrected T1-weighted images via modified unified segmentation approach, and resulting parameters were applied to the corresponding entropy maps. The normalized entropy maps were smoothed using an isotropic Gaussian filter (8 mm).

2.3.3 Background Image—A high-resolution T1-weighted image of a control subject was normalized to MNI space. This normalized image was used as the background image to overlay findings for structural identification.

2.3.4 Region-of-Interest (ROI) Analyses—Region-of-interest (ROI) analyses were performed to calculate regional brain entropy values to determine magnitude differences between groups. Using a neuromorphometric (http://www.neuromorphometrics.com) and ICBM DTI-81 [21] atlas, ROIs were created for each brain site, and these ROIs were used to create anatomic-specific masks based on findings from group comparisons. In addition, manual masks were created for sites that were not available in the atlases using the

MRIcroN. These anatomic-specific masks were used to compute average entropy values from individual smoothed maps of OSA and control subjects.

2.3.5 Statistical Analyses—The SPM12 and the IBM statistical package for social sciences (IBM SPSS v24, Armonk, New York) were employed for statistical analyses. Chi-square test and independent-samples t-tests were used to examine group differences in demographic and other data.

The smoothed entropy maps were compared voxel-by-voxel between groups using analysis of covariance (ANCOVA), with age and sex included as covariates ($p<0.005$, uncorrected). The global brain mask was used to restrict the analysis within brain regions only, and sites with significant differences between groups were overlaid onto background image for structural identification.

The mean entropy values, derived from ROI analyses, were compared between groups using ANCOVA (covariates, age and sex) and effect sizes were calculated. We considered a p-value less than 0.05 as statistically significant.

3. RESULTS

No significant differences in age ($p=0.48$), gender ($p=0.59$) or BMI ($p=0.63$) emerged between OSA and control groups (Table 1). Multiple brain areas showed reduced entropy values in OSA when compared to control subjects (Fig. 1; $p<0.005$). No brain sites showed evidence of increased entropy values in OSA children. Brain regions with reduced entropy values in OSA subjects are displayed in Fig.1 and included the insular cortices (a), external (b) and internal (c) capsules, bilateral anterior, mid, and posterior thalamus (d), anterior (s), mid (e), and posterior (f) corpus callosum, medial prefrontal cortex (g), inferior, middle and superior cerebellar peduncles (h), bilateral caudate (i), bilateral putamen (j), amygdala (k), prefrontal white matter (k), bilateral hippocampus (m), parietal cortices (n), mid (o) and posterior (p) corona radiate, occipital cortex (q), temporal white matter (r), midline and caudal pons (t), ventral medulla (u), and cerebellar cortices (v).

The regional brain entropy values from aforementioned sites are summarized in Table 2 for both OSA and control subjects, and were significantly decreased in pediatric OSA while also showing predominantly large effect sizes between groups.

4. DISCUSSION

In the present study, we report that children with OSA exhibit significantly decreased entropy values in various distinct brain anatomical sites compared to control subjects, indicating the presence of acute brain tissue changes. These changes, which are suggestive of tissue injury, appeared in brain sites underlying autonomic, cognitive, mood and respiratory functions, including the insular cortices, hippocampus, amygdala, thalamus, cingulate, and cerebellar sites. Remarkably, such observations have been previously noted in adult OSA subjects as well [22–24], suggesting that the recurrent hypoxia-re-oxygenation events, along with intermittent hypercapnia, repeated arousals, and episodic cerebral

perfusion alterations that characterize OSA may be causally implicated in such entropy brain tissue changes, which in turn may then lead to the morbid consequences of the disease.

4.1 Brain Tissue Changes versus Entropy Values

In this study, we computed entropy values from high-resolution T1-weighted images that indicate local tissue homogeneity. Extracellular water content increases in chronic disease conditions due to neuronal and axonal losses, while extracellular water decreases occur in acute conditions due to neuronal and axonal swelling and changes in tissue organization. Since entropy values varies with tissue randomness, and is affected by axonal and neuronal organization, the procedures employed herein are suitable to differentiate chronic from acute tissue changes. In previous studies conducted in adult OSA patients, in which we employed diffusion and kurtosis diffusion based procedures, our findings of reduced mean diffusivity and increased mean kurtosis values suggested that tissue injury was more likely to be acute [22, 25, 26]. However, adult patients with OSA exhibit much more frequent obstructive events and more pronounced and severe oxyhemoglobin desaturations during those events when compared to children, so it is difficult to extrapolate from studies in adults to anticipated findings in children. In the present study, we identified multiple brain regions with decreased entropy values, suggesting that despite less severe gas exchange alterations in children during obstructive respiratory events, acute changes are also occurring in pediatric OSA, possibly reflecting the unique susceptibility of the developing brain to hypoxia-reoxygenation injury [17].

4.2 Brain Changes in Pediatric OSA

Significantly decreased entropy values were detected in various brain sites, indicating acute and regionally selective neural tissue injury in children with OSA. As mentioned, the underlying mechanism for brain injury likely initiates from the upper airway collapse during sleep that promotes the occurrence of in intermittent hypoxia, leading to axonal and neuronal inflammation due to water movement from extracellular to intracellular spaces [27]. Indeed, both animal models and exosome-based experiments, as well as adult OSA studies suggest that OSA disrupts the brain blood barrier and increases its permeability [28, 29]. Thus, neuronal and axonal inflammation and increased blood brain barrier permeability may result in reduced entropy values as observed in pediatric OSA.

Reduced entropy values here were observed in the pre-frontal regions, sites that are known to regulate cognitive functions, and hence could facilitate the occurrence of behavioral deficits in OSA children [30]. Evidence of damage also appeared in the insular cortex, which is responsible for various autonomic functions, as well as emotional control, self-awareness, cognitive functioning, and motor control [31]. Of note, injury to insular cortex has been described in adult OSA patients [22, 24]. Furthermore, injury was also observed in the amygdala, a region associated with emotional function [32]. Children with OSA show reduced amygdala neural activity responses while watching empathy-eliciting scenarios, while displaying greater neural recruitment in regions implicated in cognitive control, conflict monitoring, and attentional allocation [6].

Brain damage was also observed in the thalamic regions, indicating compromised executive functions in pediatric OSA, since the thalamus acts as a critical intermediate connection between cortical and sub-cortical components, including the frontal cortex and cerebellar regions [33]. In addition, anterior, mid, posterior corpus callosum along with surrounding white matter showed tissue changes. The corpus callosum structure connects both hemispheres, and can affect a variety of functions, including executive functions, visuomotor control, autonomic regulation, and cognition [34]. Adult OSA patients have reduced regional cerebral blood flow (CBF) and altered cerebrovascular responses to hypercapnia [35]; subjects show hypoxia-induced neuronal injury in critical regions, such as cerebellum, prefrontal cortex, insula, putamen, amygdala, and hippocampus [24], regions that are vital for executive, motor, autonomic, cognitive, mood, and breathing functions [24, 36]. In addition, aberrant functional connectivity between amygdala and hippocampus is known to be present when depression is present, and children are not protected from increased risk for altered mood changes in the context of OSA [37]. Moreover, aberrant functional connectivity between hippocampus and cerebellum, along with enlargement of hippocampus have been described among OSA patients, which may lead to alterations in the memory system implicated in associative learning [38]. Both hippocampus and amygdala showed evidence of damage in our pediatric OSA patients, which might therefore underpin alterations in memory and mood systems.

Tissue changes were also observed in the temporal cortex in pediatric OSA, another region essential for cognitive function [39]. In addition, midline pons and dorsal medulla showed neural injury in pediatric OSA. Damage to these areas may underlie compromised regulation of blood pressure, respiration, and integration of baroreceptor and chemoreceptor afferents, as shown by a large body of evidence in animal studies [40]. Finally, several brain regions, including bilateral hippocampus, corpus callosum, and deep cerebellar nuclei showed neural injury that were not previously suspected in OSA children. These findings indicate that entropy procedures can be used to evaluate the nature and extent of brain changes in pediatric OSA, and are therefore worthy of expansion in future studies along with concurrent assessments of specific functional correlates.

4.3 Limitations

Several limitations of this study are worthy of mention. The sample size was relatively small, which means the group differences as reported here reflect a large effect size. A major concern that could arise from a relatively small sample size is the possibility that other brain regions with lesser magnitude of injury or greater variability in entropy changes may have not passed the relatively stringent statistical significance criteria, i.e., a β2-type error. In addition, we included images obtained in some control subject using a different MR scanner, which introduces the possibility that slight differences across instruments may adversely affect the sensitivity of detection of entropy alterations. However, we should point out that evaluation of entropy values from the two scanners were consistent, and therefore unlikely to introduce incremental inter-subject variance. Notwithstanding, it will be important to evaluate a larger cohort of children with OSA and controls to replicate current findings.

Conclusions

Entropy measures based on high-resolution T1-weighted imaging show decreased values in OSA children, indicating acute brain tissue changes. Reduced entropy values appeared in brain sites that regulate autonomic, respiratory, and cognitive functions, including the prefrontal cortices, corpus callosum, insular, frontal, temporal, hippocampus, and cerebellar areas. Multiple pathological processes, including intermittent hypoxic-re-oxygenation events and oxidative stress and inflammatory processes along with disruption of blood brain barrier integrity can contribute to the acute tissue damage. These findings reinforce the need for early detection and timely intervention in pediatric OSA in an effort to minimize the damage and optimize the repair and recovery of brain tissue in children with OSA.

Acknowledgments

This work was partially-supported by the UCLA Clinical and Translational Science Institute Research Scholar Award to RK (UL1TR001881). LKG and DG are supported by NIH grant HL-HL130984, and DG is also supported by the Herbert T. Abelson Chair in Pediatrics.

References

1. Kheirandish-Gozal L, Gozal D. Pediatric OSA Syndrome Morbidity Biomarkers: The Hunt Is Finally On! Chest. 2017; 151:500–506. [PubMed: 27720883]
2. Bixler EO, Vgontzas AN, Lin HM, Liao D, Calhoun S, Vela-Bueno A, Fedok F, Vlasic V, Graff G. Sleep disordered breathing in children in a general population sample: prevalence and risk factors. Sleep. 2009; 32:731–736. [PubMed: 19544748]
3. Kheirandish-Gozal L, De Jong MR, Spruyt K, Chamuleau SA, Gozal D. Obstructive sleep apnoea is associated with impaired pictorial memory task acquisition and retention in children. Eur Respir J. 2010; 36:164–169. [PubMed: 20075057]
4. Gozal D. Sleep-disordered breathing and school performance in children. Pediatrics. 1998; 102:616–620. [PubMed: 9738185]
5. Philby MF, Macey PM, Ma RA, Kumar R, Gozal D, Kheirandish-Gozal L. Reduced Regional Grey Matter Volumes in Pediatric Obstructive Sleep Apnea. Sci Rep. 2017; 7:44566. [PubMed: 28303917]
6. Kheirandish-Gozal L, Yoder K, Kulkarni R, Gozal D, Decety J. Preliminary functional MRI neural correlates of executive functioning and empathy in children with obstructive sleep apnea. Sleep. 2014; 37:587–592. [PubMed: 24587582]
7. Horne RSC, Roy B, Walter LM, Biggs SN, Tamanyan K, Weichard A, Nixon GM, Davey MJ, Ditchfield M, Harper RM, Kumar R. Regional Brain Tissue Changes and Associations with Disease Severity in Children with Sleep Disordered Breathing. Sleep. 2017
8. Gozal D. CrossTalk proposal: the intermittent hypoxia attending severe obstructive sleep apnoea does lead to alterations in brain structure and function. J Physiol. 2013; 591:379–381. [PubMed: 23322286]
9. Gozal E, Row BW, Schurr A, Gozal D. Developmental differences in cortical and hippocampal vulnerability to intermittent hypoxia in the rat. Neurosci Lett. 2001; 305:197–201. [PubMed: 11403939]
10. Macey PM, Kheirandish-Gozal L, Prasad JP, Ma RA, Kumar R, Philby MF, Gozal D. Altered Regional Brain Cortical Thickness in Pediatric Obstructive Sleep Apnea. Front Neurol. 2018; 9:4. [PubMed: 29403430]
11. Maani R, Yang YH, Emery D, Kalra S. Cerebral Degeneration in Amyotrophic Lateral Sclerosis Revealed by 3-Dimensional Texture Analysis. Front Neurosci. 2016; 10:120. [PubMed: 27064416]
12. Kassner A, Thornhill RE. Texture analysis: a review of neurologic MR imaging applications. Am J Neuroradiol. 2010; 31:809–816. [PubMed: 20395383]

13. Gladyshev GP. Thermodynamic theory of biological evolution and aging. Experimental verification of the theory. Izv Akad Nauk Ser Biol. 2000:261–268.
14. Zhang Y, Zhu H, Mitchell JR, Costello F, Metz LM. T2 MRI texture analysis is a sensitive measure of tissue injury and recovery resulting from acute inflammatory lesions in multiple sclerosis. Neuroimage. 2009; 47:107–111. [PubMed: 19361563]
15. Montgomery-Downs HE, O'Brien LM, Gulliver TE, Gozal D. Polysomnographic characteristics in normal preschool and early school-aged children. Pediatrics. 2006; 117:741–753. [PubMed: 16510654]
16. Berry RB, Budhiraja R, Gottlieb DJ, Gozal D, Iber C, Kapur VK, Marcus CL, Mehra R, Parthasarathy S, Quan SF, Redline S, Strohl KP, Ward SL Davidson, Tangredi MM, M. American Academy of Sleep. Rules for scoring respiratory events in sleep: update of the 2007 AASM Manual for the Scoring of Sleep and Associated Events. Deliberations of the Sleep Apnea Definitions Task Force of the American Academy of Sleep Medicine. J Clin Sleep Med. 2012; 8:597–619. [PubMed: 23066376]
17. Gozal D, Crabtree VM, Capdevila O Sans, Witcher LA, Kheirandish-Gozal L. C-reactive protein, obstructive sleep apnea, and cognitive dysfunction in school-aged children. Am J Respir Crit Care Med. 2007; 176:188–193. [PubMed: 17400731]
18. Barnes ME, Gozal D, Molfese DL. Attention in children with obstructive sleep apnoea: an event-related potentials study. Sleep Med. 2012; 13:368–377. [PubMed: 22425681]
19. Rorden C, Karnath HO, Bonilha L. Improving lesion-symptom mapping. J Cogn Neurosci. 2007; 19:1081–1088. [PubMed: 17583985]
20. Ashburner J, Friston KJ. Unified segmentation. Neuroimage. 2005; 26:839–851. [PubMed: 15955494]
21. Mori S, Oishi K, Jiang H, Jiang L, Li X, Akhter K, Hua K, Faria AV, Mahmood A, Woods R, Toga AW, Pike GB, Neto PR, Evans A, Zhang J, Huang H, Miller MI, van Zijl P, Mazziotta J. Stereotaxic white matter atlas based on diffusion tensor imaging in an ICBM template. Neuroimage. 2008; 40:570–582. [PubMed: 18255316]
22. Kumar R, Chavez AS, Macey PM, Woo MA, Yan-Go FL, Harper RM. Altered global and regional brain mean diffusivity in patients with obstructive sleep apnea. J Neurosci Res. 2012; 90:2043–2052. [PubMed: 22715089]
23. Kumar R, Pham TT, Macey PM, Woo MA, Yan-Go FL, Harper RM. Abnormal myelin and axonal integrity in recently diagnosed patients with obstructive sleep apnea. Sleep. 2014; 37:723–732. [PubMed: 24899761]
24. Macey PM, Henderson LA, Macey KE, Alger JR, Frysinger RC, Woo MA, Harper RK, Yan-Go FL, Harper RM. Brain morphology associated with obstructive sleep apnea. Am J Respir Crit Care Med. 2002; 166:1382–1387. [PubMed: 12421746]
25. Tummala S, Palomares J, Kang DW, Park B, Woo MA, Harper RM, Kumar R. Global and Regional Brain Non-Gaussian Diffusion Changes in Newly Diagnosed Patients with Obstructive Sleep Apnea. Sleep. 2016; 39:51–57. [PubMed: 26285005]
26. Tummala S, Roy B, Park B, Kang DW, Woo MA, Harper RM, Kumar R. Associations between brain white matter integrity and disease severity in obstructive sleep apnea. J Neurosci Res. 2016; 94:915–923. [PubMed: 27315771]
27. Tauman R, Ivanenko A, O'Brien LM, Gozal D. Plasma C-reactive protein levels among children with sleep-disordered breathing. Pediatrics. 2004; 113:e564–569. [PubMed: 15173538]
28. Palomares JA, Tummala S, Wang DJ, Park B, Woo MA, Kang DW, St Lawrence KS, Harper RM, Kumar R. Water Exchange across the Blood-Brain Barrier in Obstructive Sleep Apnea: An MRI Diffusion-Weighted Pseudo-Continuous Arterial Spin Labeling Study. J Neuroimaging. 2015; 25:900–905. [PubMed: 26333175]
29. Khalyfa A, Gozal D, Kheirandish-Gozal L. Plasma Exosomes Disrupt the Blood-Brain Barrier in Children with Obstructive Sleep Apnea and Neurocognitive Deficits. Am J Respir Crit Care Med. 2018; 197:1073–1076. [PubMed: 29053009]
30. Beebe DW, Gozal D. Obstructive sleep apnea and the prefrontal cortex: towards a comprehensive model linking nocturnal upper airway obstruction to daytime cognitive and behavioral deficits. J Sleep Res. 2002; 11:1–16.

31. Craig AD. How do you feel–now? The anterior insula and human awareness. Nat Rev Neurosci. 2009; 10:59–70. [PubMed: 19096369]
32. Phelps EA, LeDoux JE. Contributions of the amygdala to emotion processing: from animal models to human behavior. Neuron. 2005; 48:175–187. [PubMed: 16242399]
33. Beebe DW, Groesz L, Wells C, Nichols A, McGee K. The neuropsychological effects of obstructive sleep apnea: a meta-analysis of norm-referenced and case-controlled data. Sleep. 2003; 26:298–307. [PubMed: 12749549]
34. Schulte T, Muller-Oehring EM. Contribution of callosal connections to the interhemispheric integration of visuomotor and cognitive processes. Neuropsychol Rev. 2010; 20:174–190. [PubMed: 20411431]
35. Balfors EM, Franklin KA. Impairment of cerebral perfusion during obstructive sleep apneas. Am J Respir Crit Care Med. 1994; 150:1587–1591. [PubMed: 7952619]
36. Macey PM, Woo MA, Macey KE, Keens TG, Saeed MM, Alger JR, Harper RM. Hypoxia reveals posterior thalamic, cerebellar, midbrain, and limbic deficits in congenital central hypoventilation syndrome. J Appl Physiol (1985). 2005; 98:958–969. [PubMed: 15531561]
37. Crabtree VM, Varni JW, Gozal D. Health-related quality of life and depressive symptoms in children with suspected sleep-disordered breathing. Sleep. 2004; 27:1131–1138. [PubMed: 15532207]
38. Rosenzweig I, Kempton MJ, Crum WR, Glasser M, Milosevic M, Beniczky S, Corfield DR, Williams SC, Morrell MJ. Hippocampal hypertrophy and sleep apnea: a role for the ischemic preconditioning? PLoS One. 2013; 8:e83173. [PubMed: 24349453]
39. Bunce D, Anstey KJ, Cherbuin N, Burns R, Christensen H, Wen W, Sachdev PS. Cognitive deficits are associated with frontal and temporal lobe white matter lesions in middle-aged adults living in the community. PLoS One. 2010; 5:e13567. [PubMed: 21042415]
40. Gozal D, Daniel JM, Dohanich GP. Behavioral and anatomical correlates of chronic episodic hypoxia during sleep in the rat. J Neurosci. 2001; 21:2442–2450. [PubMed: 11264318]

Highlights

- We assess nature and extent of tissue changes in pediatric OSA.
- Pediatric OSA show acute injury in cognitive, mood, and autonomic sites.
- OSA subjects have structural basis for cognitive and behavioural deficits.

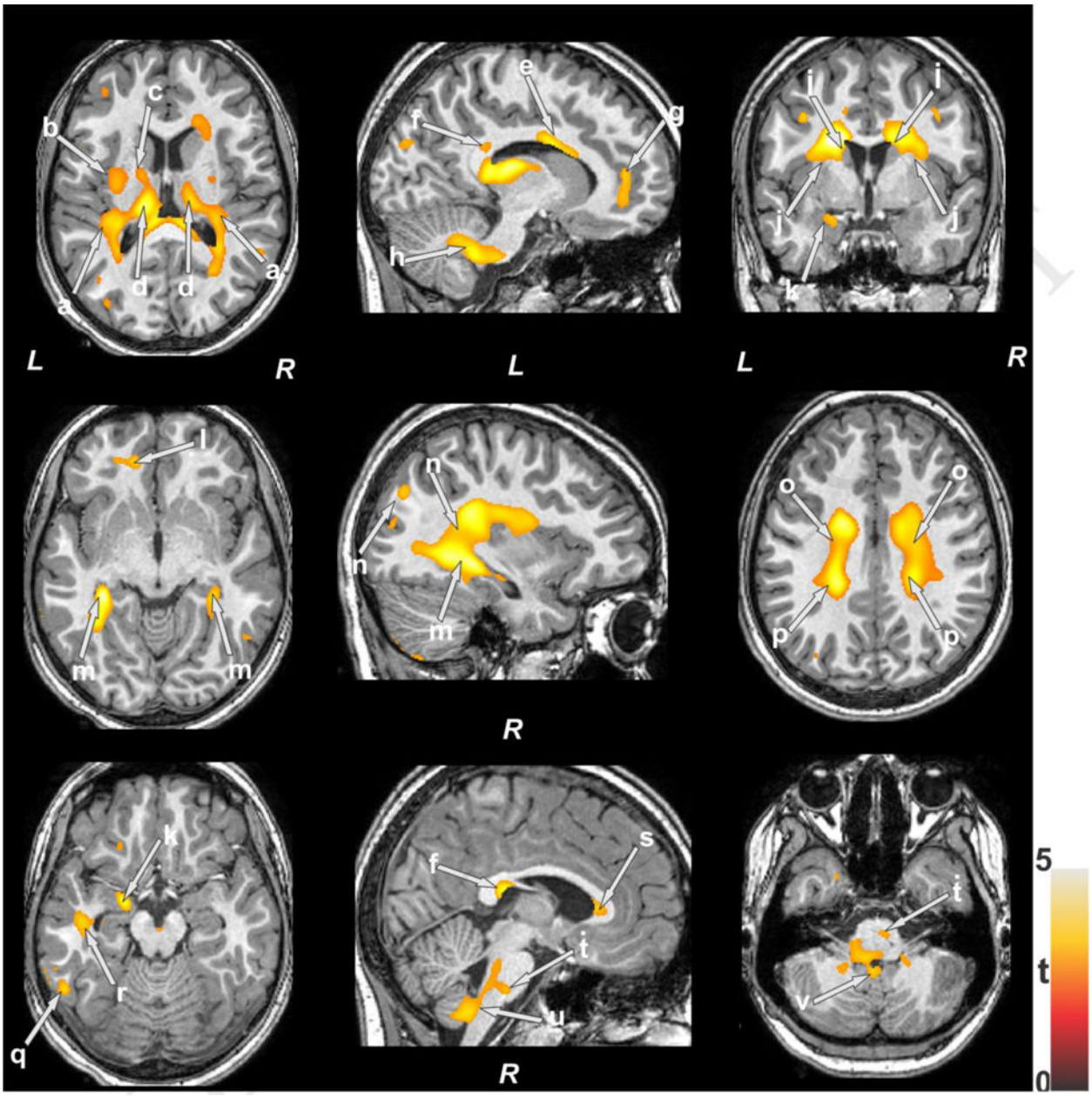

Figure 1.

Brain sites showing lower entropy in OSA compared to control subjects. These sites included the insular cortices (a), external (b) and internal (c) capsules, bilateral anterior, mid, and posterior thalamus (d), anterior (s), mid (e), and posterior (f) corpus callosum, medial prefrontal cortex (g), inferior, middle, and superior cerebellar peduncles (h), bilateral caudate (i), bilateral putamen (j), amygdala (k), prefrontal white matter (k), bilateral hippocampus (m), parietal cortices (n), mid (o) and posterior (p) corona radiate, occipital cortex (q), temporal white matter (r), midline and caudal pons (t), ventral medulla (u), and cerebellar cortices (v). Color bar represents t-statistic values (*L = Left; R = Right*).

Table 1

Demographic and relevant clinical and polysomnographic variables in children with OSA and control subjects.

Variables	Control (mean ± SD) [n = 8]	OSA (mean ± SD) [n = 10]	P-value
Age (years)	8.8±1.6	7.9±1.1	0.487
Gender (Male: Female)	5:3	5:5	0.596
BMI (kg/m^2)	19.59 ± 5.9	20.89 ± 6.7	0.676
AHI (events/hour)	0.76 ± 0.51 (n = 5)	8.87 ± 2.9	< 0.001

Table Legend: OSA: obstructive sleep apnea, SD: standard deviation, L: Left, R: Right.

Table 2

Regional brain entropy values in controls and pediatric OSA subjects.

Brain region	Control (mean ± SD) N = 8	OSA (mean ± SD) N = 10	Cluster Size (voxels)	P-value (effect size)
L Insula	0.83 ± 0.02	0.79 ± 0.02	63	0.012 (1.99)
L Putamen	0.79 ± 0.03	0.75 ± 0.03	50	0.017 (1.33)
R Caudate	0.84 ± 0.02	0.79 ± 0.02	324	0.002 (2.50)
L Caudate	0.85 ± 0.02	0.81 ± 0.02	585	0.001 (1.99)
R Thalamus	0.81 ± 0.02	0.76 ± 0.02	1500	0.003 (2.50)
L Thalamus	0.82 ± 0.02	0.77 ± 0.02	3087	0.008 (2.49)
R Hippocampus	0.87 ± 0.01	0.83 ± 0.01	545	0.001 (4.00)
L Hippocampus	0.86 ± 0.01	0.83 ± 0.01	819	0.001 (3.00)
L Amygdala	0.84 ± 0.02	0.80 ± 0.02	552	0.004 (1.99)
L Medial Orbital gyrus	0.87 ± 0.01	0.84 ± 0.01	55	0.002 (3.00)
R Superior Parietal	0.84 ± 0.02	0.80 ± 0.02	125	0.004 (1.99)
L Temporal Pole	0.87 ± 0.01	0.84 ± 0.01	129	0.006 (3.00)
L Medial Frontal Cortex	0.84 ± 0.02	0.81 ± 0.02	18	0.007 (1.49)
Corpus Callosum	0.82 ± 0.02	0.78 ± 0.02	3612	0.002 (1.99)
L Cerebellar Peduncle	0.84 ± 0.01	0.81 ± 0.01	321	0.006 (2.99)
L Posterior Limb of Internal Capsule	0.85 ± 0.01	0.82 ± 0.01	472	0.005 (3.00)
R Anterior Corona Radiata	0.87 ± 0.02	0.83 ± 0.02	779	0.005 (2.00)
L Anterior Corona Radiata	0.86 ± 0.02	0.82 ± 0.02	1459	0.005 (2.00)
R Superior Corona Radiata	0.81 ± 0.03	0.76 ± 0.03	1758	0.009 (1.66)
L Superior Corona Radiata	0.81 ± 0.02	0.76 ± 0.02	2720	0.008 (2.50)
R Posterior Corona Radiata	0.78 ± 0.03	0.72 ± 0.03	1015	0.013 (2.00)
L Posterior Corona Radiata	0.80 ± 0.03	0.74 ± 0.03	361	0.013 (2.00)
L External Capsule	0.85 ± 0.02	0.83 ± 0.02	22	0.003 (1.00)
Cerebellar Cortices	0.84 ± 0.02	0.80 ± 0.02	1110	0.004 (1.99)
Ventral Medulla	0.87 ± 0.01	0.84 ± 0.01	812	0.003 (3.00)
Pons	0.82 ± 0.02	0.77 ± 0.02	2679	0.007 (2.49)

Table legend: SD, standard deviation; BMI, body mass index; AHI, apnea hypopnea index.